

Soft X-ray Monochromators for Third-Generation Undulator Sources

H. A. Padmore and T. Warwick

Advanced Light Source, Accelerator and Fusion Research Division, Lawrence Berkeley Laboratory, Berkeley, CA 94720, USA

(Received 2 June 1994; accepted 17 June 1994)

Over the past ten years, the resolving power from new designs of bending-magnet-based soft X-ray monochromators has increased by more than an order of magnitude. This has led to a revolution in soft X-ray spectroscopy, but the limited flux at this high resolution has allowed only relatively efficient measurements to be made, such as photo-absorption. Application of this new tool of high-resolution spectroscopy to photoemission, energy-resolved fluorescence spectroscopy and microscopy has now been made possible with the advent of undulator sources of soft X-rays. Here we have reviewed the recent development of undulator-based soft X-ray monochromators, the special features of undulators in general and the resulting benefits and problems, and describe the state of the art undulator beamline, 7.0 at the Advanced Light Source. In addition, we offer some speculation as to the possible routes to the next or ultimate generation of soft X-ray monochromator.

Keywords: soft X-rays; monochromators; undulators; X-ray spectroscopy; microscopy.

1. Introduction

The development in soft X-ray monochromator design and performance over the past ten years has been dramatic. We have gone from a situation where the average monochromator of the early 1980s had a resolving power of less than 500 to the state of the art systems of today in which resolving powers of 10^4 are routine. In addition, the flux output has increased by two to three orders of magnitude and the brightness by four to five orders of magnitude. These dramatic improvements have resulted from three parallel developments: improved fabrication techniques for low slope error optical components, the construction of monochromators based on decoupled focusing schemes and the use of undulators on low-emittance storage rings.

In the late 1980s, the first two developments had matured and a new generation of high-resolution spectroscopic techniques was born. The flux available at this newly achieved high resolution was sufficient for techniques such as photo-absorption, in which the detection methods are inherently efficient, but was insufficient for the more sophisticated techniques such as photo-emission and fluorescence spectroscopy and microscopy.

The advent of undulator beams from a new generation of ultra-high brightness soft X-ray sources, such as the Advanced Light Source (ALS) at Berkeley and ELETTRA at Trieste, has enabled the problem of insufficient flux to be overcome, but at the cost of significantly more sophisticated instrumentation. The properties of undulators that lead to the enormous gains in resolved flux and brightness also lead to problems of high thermal load on the beamline components and necessitate a radically new approach to instrument design. The very small phase-space volume

occupied by the source also dictates that the beam and beamline must be highly stable. This has required the development of beam-position monitors that can work in the intense raw undulator light as well as optical systems that are thermally and vibrationally stable to high precision. The single most radical departure from traditional design has been the need to use actively cooled optical components whilst at the same time improving the slope error over that previously available in traditional materials such as fused quartz. In many cases this has involved the use of integrally cooled metal optics; this has in turn substantially increased the mass of the optical systems and hence traditional methods of mounting optics have had to be abandoned in favor of more substantial and complex systems.

In this paper we will review some of the salient features of the development of soft X-ray undulator-based monochromators and give a description of the state of the art system at the ALS, beamline 7.0 (Warwick & Heimann, 1992; Warwick, Heimann, Mossessian, McKinney & Padmore, 1994). We will first, however, briefly review the special properties of undulator light that give us both opportunities and problems.

2. Characteristics of undulator sources

A full description of the properties of undulator light is beyond the scope of this article, but we will lay out the most important features that determine the design of optical systems. Undulator radiation is generated by a relativistic electron beam being deflected by a periodic magnetic field. The oscillation of period λ_u (cm) caused by the magnetic field of peak strength B_0 (T) can be characterized by a

deflection parameter K given by,

$$K = 0.93\lambda_u B_0.$$

This parameter is important because it characterizes the angular deflection of the beam $\delta = K/\gamma$, where γ is the electron energy in units of the rest mass energy. For an undulator, K is typically near unity and therefore the horizontal angular radiation width is rather small; a $K = 1$ undulator on a machine at 1.5 GeV gives a fan width of ± 0.33 mrad. The interference generated by the emission of light from each pole leads to a harmonic spectrum in which the harmonic energies, ε_n (eV) can be expressed as,

$$\varepsilon_n = 950[E^2/(1+K^2/2)\lambda_u],$$

where E (GeV) is the electron energy and λ_u is the undulator period. The r.m.s. angular divergence $\sigma_{r'}$ and the r.m.s. beam size σ_r of the diffraction-limited central cone of radiation, at the harmonic wavelength λ_n for an undulator of length L can be given by,

$$\begin{aligned}\sigma_{r'} &= (\lambda_n/L)^{1/2}, \\ \sigma_r &= (\lambda L/4\pi)^{1/2}.\end{aligned}$$

For example, for a 5 m undulator radiating at the carbon K edge, 44 Å, the diffraction-limited r.m.s. divergence and beam size of the central cone is 30 μ rad and 12 μ m, respectively. In comparison to the vertical angular divergence from a typical bending-magnet source, this value is about one order of magnitude lower. At the third-generation storage rings, the electron beam contributes only a very small increase to the vertical divergence of the undulator beams; for example, at the ALS the r.m.s. divergence of the beam in the vertical direction is less than 10 μ rad. As the aberrations of optical systems are a strong function of aperture, the extremely low value of divergence allows us to manipulate the beam, for example by demagnifying, without the normal penalty of producing aberrations. An example of such a scheme is in production of a demagnified image of the source at the entrance slit of a monochromator. This improves the throughput at high resolution, corresponding to small slit sizes, without either producing excessive aberration at the slit or at the grating downstream. The measured vertical source size in an insertion device straight at the ALS is < 40 μ m, and combined with the low divergence allows us to demagnify the beam to a size of less than 4 μ m r.m.s., thus allowing us to operate at very high resolution without the normal quadratic loss of flux given by closing both the entrance and exit slits.

As an undulator consists of many periods radiating coherently, the flux directed into the central radiation cone can be very high. An approximate formula for this flux is given below,

$$F_n = 1.43 \times 10^{14} N Q_n I,$$

where Q_n is the function of K shown in Fig. 1, N is the number of periods, and I is the beam current (A). For

the 89-period, 5 cm period length ALS undulator U5, at a deflection parameter K of 1, the flux radiated in the central cone at the standard operating current of 400 mA is 3×10^{15} photons s^{-1} in a 0.1% bandwidth.

The combination of a small source size, small divergence and extremely high flux in the central radiation cone results in an overall enhancement in flux throughput over monochromators on bending-magnet sources of typically three to four orders of magnitude.

The penalty that comes with the use of undulators is in high power loading on the beamline components (Avery, 1984). For an undulator of length L (m), the total power P (W), the vertically integrated horizontal angular power density P' (W mrad $^{-1}$) and the central angular power density P'' (W mrad $^{-2}$) can be given by,

$$\begin{aligned}P &= 633E^2 B_0^2 L I, \\ P' &= 8.66E^3 B_0 I N, \\ P'' &= 10.84E^4 B_0 I N.\end{aligned}$$

As an example, an ALS 5 cm period undulator with 89 periods operating at the carbon K edge, $K = 1$, would radiate a total power of 115 W, with a horizontal angular power density of 218 W mrad $^{-1}$ and a central power density of 410 W mrad $^{-2}$. As shown above, the r.m.s. angular width of the central radiation cone would be 30 μ rad, compared with the angular deviation of the electron beam and hence the horizontal width of the radiation fan, of 0.34 mrad (half width). The power falling on the optics can therefore be significantly reduced by use of a horizontal aperture, in the case above reducing the power transmitted to the first optical element by one order of magnitude. It can be seen from the form of Fig. 1 that at a K of

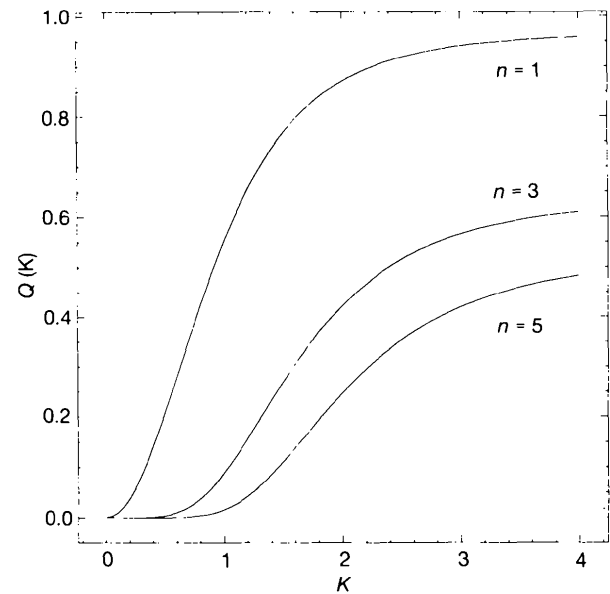


Figure 1

The function $Q(K)$, where K is the undulator deflection parameter. The function is directly related to the flux radiated in the central cone. Functions for the first, third and fifth harmonics are shown.

1, the undulator spectrum will be dominated by the first harmonic. As an example of a strong field undulator, the ALS 5 cm period undulator will be able to be used with a minimum gap of 1.4 cm. This corresponds to a fundamental of 51 eV, a peak on-axis field of 0.82 T and a K of 3.82. In this case we will have P , P' and P'' of 1723 W, 853 W mrad⁻¹ and 1602 W mrad⁻², respectively, an r.m.s. central cone angular width of 73 μ rad, and a maximum horizontal angular deflection of 1.3 mrad.

Because of the very large total power radiated, it is clearly essential to reduce this to an acceptable level by reducing the horizontal aperture. The central power density scales as K^2 , and in the K range given above increases by a factor of 14. Operation at high K values is necessary to give a reasonable photon energy tuning range in the fundamental, and so that sufficient power will be radiated in the higher harmonics to further extend the range of a single device operating at a fixed electron energy. The thermal distortion suffered by an optical element can be generally viewed as two parts, a general overall bending caused by thermal gradients within the substrate, and non-uniform expansion of the element local to the heated surface (Smither *et al.*, 1989). Although the total power can be reduced by aperturing, the on-axis power density is determined by the electron energy and K . With a vertically reflecting and focusing geometry, as the power distribution is much wider than the central cone region, using a horizontal aperture with no vertical restriction results in a significant reduction in total power absorbed by the mirror, but gives only a slow change in power in the vertical focusing direction, and hence a low slope error. Vertical aperturing for a vertical reflection, however, would lead to a rapid change in heating along the length of the mirror and, therefore, to the generation of slope errors. The further reduction of thermally generated slope errors to acceptable values must be accomplished by the adoption of actively cooled components. This has meant that components have to be modeled using finite-element methods, and in the case of the ALS has resulted in the adoption of metal optics in which the cooling channels are located a few millimetres from the optical surface (DiGennaro *et al.*, 1988; DiGennaro & Swain, 1990*a,b*). The adoption of integrally cooled metal optics has implications for the whole beamline design, due to the large mass of the optical element, the need for stress-free mounting, and the necessity of using a construction in which a guard vacuum separates the water-cooled area from the ultra-high-vacuum enclosure. Aspects of these considerations will be described in §4, applied to ALS undulator beamline 7.0.

3. An overview of undulator monochromators

Before describing in detail the construction and operation of beamline 7.0, it is worthwhile to review briefly the rapid evolution of undulator-based monochromators. Our intention here is not to be comprehensive, but rather to give a general overview of the progression of the field.

In addition, for brevity we will not cover the development of Rowland-circle monochromators but concentrate on plane-grating monochromators and non-Rowland spherical grating monochromators. Rowland-circle designs have, however, reached excellent resolving powers, in principle have large dispersive acceptance, and embody many interesting features. In particular the 10 m monochromator at the Photon Factory (Maezawa *et al.*, 1986) has been successfully used on a 60-period undulator source at high resolution (Yagashita, Masui, Toyoshima, Maezawa & Shigemasa, 1992). In addition, a modification of this design by Muramatsu & Maezawa (1989) and Muramatsu, Kato, Maezawa & Harada (1992) in which the instrument was used without an entrance slit is interesting as the pre-mirror and grating were used in a coma-correcting pair using the method developed by Namioka, Noda, Goto & Katayama (1983).

Many monochromator designs in the early 1980s had shown excellent theoretical performance, only to demonstrate poor experimental performance. The main reasons for this divergence between theory and reality were firstly the systems were often optically complex and difficult to align, and more importantly, they used off-axis elements that were difficult to fabricate. The first design which proposed a simple configuration in which the high-quality optics necessary were readily available was the spherical grating monochromator (SGM) (Hogrefe, Howells & Hoyer, 1986; Padmore, 1986*a,b*; Chen, 1987), in which a single spherical grating was used between the entrance and exit slits of a fixed included-angle configuration. Wavelength scanning was accomplished by simple rotation of the grating, and the focus condition was satisfied by translation of the exit slits. The demonstration of a resolving power of near 10^4 in the soft X-ray region by Chen & Sette (Chen & Sette, 1989, 1990) on a bending-magnet beamline revolutionized the field of soft X-ray research and led to the SGM becoming the standard design for high-resolution spectroscopy.

In a parallel development, the plane-grating monochromator was being developed by Petersen, from the multi-deviation angle design of Flipper (Senf *et al.*, 1986), and from the earlier design of Gleispimo (Kunz, Haensel & Sonntag, 1968; Dietrich & Kunz, 1972). This design, known as the SX700 (Petersen, 1982, 1986; Petersen, Haase, Puschmann, Reimer & Treichler, 1983), employed a plane pre-mirror, a plane grating and an ellipsoidal mirror in a vertically dispersing geometry. The new feature of the design was that the pre-mirror and grating were independently rotatable, allowing solution of the focusing condition for any wavelength by the selection of the correct included angle on the grating. In effect, the virtual focus of the grating could be located at the object position defined by the ellipsoid and exit slit. A further significant benefit of the design was that by a correct choice of this fixed virtual object position, and hence defining the relationship between the included angle and wavelength, the conditions for the maximum efficiency of the grating were approximately met. This meant that with only one grating, the monochromator

could tune from the VUV to the upper end of the soft X-ray energy region. As there was a free selection of the deviation angle for any wavelength if the focus condition was abandoned, the design also allowed the suppression of high-order radiation by use of smaller included angles. The problem of rotation and translation of the pre-mirror was elegantly solved (Reimer & Torge, 1983) by use of an off-axis rotation scheme that closely approximated the required translation. Although the resolution achieved by the early versions of the instrument were hindered by the figure errors of the ellipsoidal focusing mirror, these problems have been recently corrected with the successful fabrication of mirrors with less than $2 \mu\text{rad}$ r.m.s. slope error, and resolving powers of around 10^4 have been achieved (Domke *et al.*, 1992; Kaindl, Domke, Laubschat, Weschke & Xue, 1992). A full description of the development of the SX700 has been given by Petersen, Jung, Hellwig, Peatman & Gudat (1994).

Both the SGM and SX700 designs have been developed further, firstly with their application to undulator sources and secondly in modification of their basic design. In the case of the SGM, the main problems with the original design are movement of the exit slit as a function of wavelength, thereby causing an imaging problem for following optical elements, lack of a mechanism for higher order suppression and the need for many gratings to cover a wide wavelength region adequately. These problems have essentially been solved by inclusion of a variable-angle pre-mirror as in the SX700 (Padmore, 1989, 1991). An appropriate included angle can be found as a function of wavelength so that the entrance and exit slits can remain in fixed positions and, by use of different radii for different gratings, widely differing average included angles can be used for each wavelength range covered by each grating. This idea of included-angle ranges for optimum performance originates in the multi-angle designs of Flipper at HASYLAB (Senf *et al.*, 1986) and TGM5 at BESSY (Peatman *et al.*, 1989). This design has now also been applied to undulators constructed at BESSY (Peatman, Bahrtdt, Eggenstein & Senf, 1991; Peatman, Bahrtdt, Gaupp, Schafers & Senf, 1992) and at ELETTRA (Nataletti *et al.*, 1992). A comprehensive description of this class of monochromator, and in particular its application to microscopy, has been given by Jark & Melpignano (1994).

The standard SGM design has been used on multipole wiggler beamlines such as beamline 6 at SSRL (Heimann *et al.*, 1990) and on soft X-ray undulators such as those at the Brookhaven NSLS for microscopy (X1A) (Buckley *et al.*, 1989) and spectroscopy (X1B) (Randall, Eberhardt *et al.*, 1992; Randall, Feldhaus *et al.*, 1992). All of these designs have come near their design goal in terms of ultimate resolution.

The original design of the SX700 has been modified by a number of groups, both to improve the optical performance and make the design suitable for use with an undulator source. One of the problems that resulted from separation of the real source and virtual sources was that the ellipsoid focused light to an astigmatic monochromatic focal plane. Lines of constant wavelength on the focal plane were curved, necessitating the use of curved slits. In order to overcome this problem, the focusing was separated into two orthogonal elliptical cylinders, the first upright cylinder in front of the monochromator collecting radiation and focusing it in the horizontal direction onto the sample, and the second element replaced the normal ellipsoid and focused light from the virtual source onto the exit slit (Nyholm, Svensson, Nordgren & Flodstrom, 1986). A second solution was to replace the ellipsoid by a spherical mirror. This solution, first proposed by Padmore (Padmore, 1989; Mythen, van der Laan & Padmore, 1992) and later by Reininger & Saile (1990) both for undulator sources, required the use of a demagnification much less than in the ellipsoidal mirror version of the SX700 in order to avoid coma. The demagnification was adjusted so that the aberration-limited resolution was a small fraction of the source-size-limited resolution, and resulted in a large image distance. Spherical mirrors are much easier to fabricate than ellipsoids, and as there is no symmetry axis as with the ellipsoid that must pass through the source, the geometry is insensitive to source steering errors. A further advantage of the spherical mirror design is that the image and object distances are no longer fixed by the geometry of the mirror as with an elliptical shape. A movement of the exit-slit position corresponds to a required movement of the virtual source position, *i.e.* the fixed-focus condition can be varied. This can be used to vary the balance between flux throughput and resolution. For example, at a particular wavelength, the included angle could be increased, thus

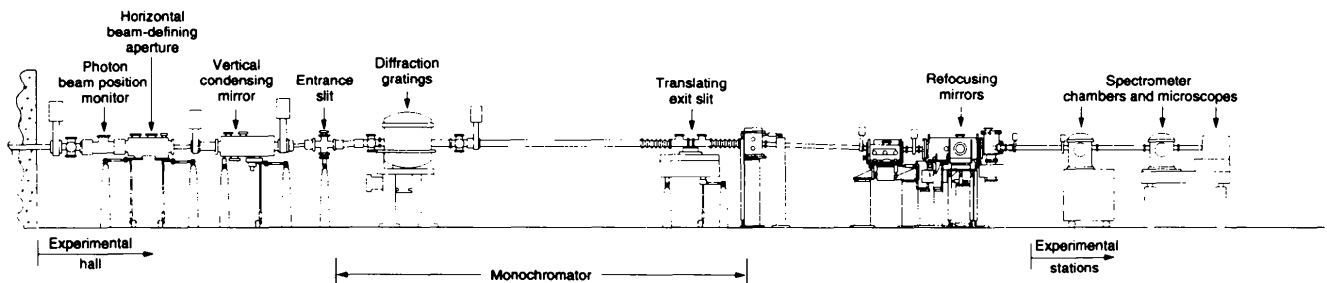


Figure 2
Beamline layout of ALS undulator beamline 7.0.

reducing the angle of incidence on the grating and hence improving the source-size-limited resolution. This would be at the expense of a lower vertical aperture and hence a lower fraction of the light would be collected in the monochromator aperture. In practice, the monochromator constant relating the virtual image to real object distance, can be changed by over a factor of 5, resulting in the same range of source-size-limited resolution. This elegant method of changing resolution has been successfully used at DORIS (Larsson *et al.*, 1992) on a bypass undulator, and at BESSY on a bending magnet (HEPGM3) (Petersen, Jung, Hellwig, Peatman & Gudat, 1992). A further modification of the basic design was proposed in which the monochromator is used with an entrance slit, and a pre-mirror system is used to arrange for the virtual image in the dispersive plane to lie on top of the real object in the non-dispersive plane (Jark, 1992; Lu & Chen, 1991). In addition, Jark (1992) proposed using the ellipsoidal mirror rotated by 90° , so that the focusing was performed by the sagittal curvature. In this way the resolution-determining slope errors in the sagittal direction are reduced by the sine of the grazing incidence angle. This solution was also proposed for the pre-mirror in order to reduce the slope error tolerance required due to thermal distortion. This monochromator is in use on Ultra-ESCA undulator beamline at ELETTRA.

4. Undulator beamline 7.0 at the ALS

Beamline 7.0 at the ALS has a 5 cm period undulator with 89 periods providing light from 60 to 1200 eV using the first, third and fifth harmonics (Hoyer *et al.*, 1992). The beamline outside the shield wall is shown schematically in Fig. 2. The main components are a pair of photon beam-position monitors (PBPM), a horizontal beam-defining aperture (HBDA) and the beamline optics. The first mirror images the vertical source onto the monochromator entrance slit, which serves as an object that is imaged and dispersed by the grating to the exit slit. Refocus optics generate a small spot of monochromatic light at the experiment.

The PBPM is shown in Fig. 3 and is based on previous undulator monitor designs (Mortazavi, Woodle, Rarback, Shu & Howells, 1986; Johnson & Oversluizen, 1989), and a prototype built at the ALS and tested at the NSLS (Warwick, Shu, Rodricks & Johnson, 1992). The first monitor uses two blades that penetrate into the edges of the beam, and vertical position is inferred from the difference/sum of the photoemitted currents from the blades. The blades themselves are copper, water cooled *via* thin electrically insulating but thermally conducting sapphire sheets. Extraction plates at the top and bottom of the blade assembly are used as bias electrodes to sink photoemitted current. The second monitor has blades at 45° for sensing both the horizontal and vertical direction out of the shadow of the first monitor. In the vertical direction, the two monitor signals are used together to derive the position and angle of the beam at the source and provide an error signal

for a stability feedback loop. First measurements of beam stability using these detectors show excellent performance of the storage ring, with stability in vertical position and angle at a level $10\times$ smaller than the size and divergence of the electron beam.

The HBDA employs grazing incidence (7°) blades to reduce the total power falling on the optical elements as described previously. Its aperture can be adjusted and its horizontal position can be scanned under computer control to locate the central cone.

The beam is then vertically deflected and focused at 15:1 demagnification by a water-cooled spherical mirror at a grazing angle of 2° onto the entrance slits of the monochromator. The mirror is integrally water cooled and its grazing angle can be changed either by manual control, or using a piezo driver under computer control. The mirror tank also contains fixed vertical defining apertures to ensure that the beam can only intersect with the mirror surface.

The entrance slits assembly is machined from a single block of Glidcop, a dispersion-strengthened copper alloy (SCM Metal Products Inc., 11000 Cedar Avenue, Cleveland, OH 44106, USA). This alloy is used for all the high-stress applications such as integrally cooled optics (DiGennaro & Swain, 1990*b*), slits and beam-defining apertures. The machining of the copper block to provide the

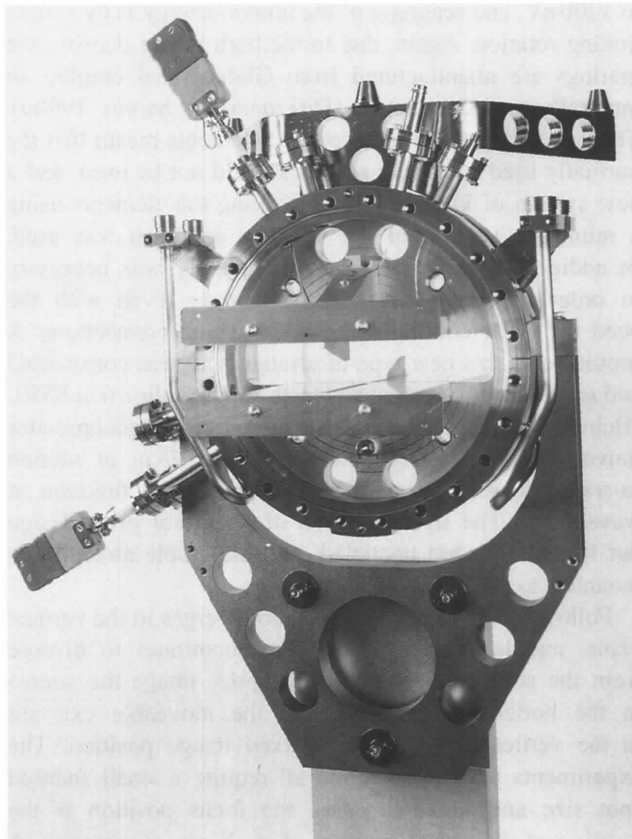


Figure 3 Vertical photon-beam-position monitor (PBPM) showing the two vertical water-cooled sensing blades.

necessary bilateral motion of the slit jaws is accomplished using wire electric discharge machining (wire EDM) and is combined with an efficient cooling scheme. This ensures that the expansion or motion of the slit jaws under full power load is less than a few micrometers. This is essential as the slit width for operation of the monochromator at the highest resolution is typically $10\ \mu\text{m}$. The slit assembly is mounted on Invar struts to a thermally stabilized base.

The use of a six-strut mounting scheme for all the beamline components, the use of Invar for the critical components, and the use of thermally stabilized mounting structures is common to all of the beamline design. Three struts support the structure in the vertical direction and three in the horizontal plane. This has proven to be immensely successful, giving structures that are easy to survey into position, are extremely stable, and have a high first resonant frequency of typically greater than 30 Hz. The beamline is designed to achieve the maximum transmission of usable light into the monochromator, and because of the low divergence of the undulator light, the small source size and the high demagnification, the throughput is 100% for slits wider than $20\ \mu\text{m}$; this width is typical for high-resolution operation.

Following the entrance slit, the beam diverges onto one of three gratings which are selectable by lateral translation. Spherical gratings are employed with groove frequencies of 150, 380 and $925\ \text{l mm}^{-1}$ to cover the energy range from 60 to 1200 eV, and scanning of the photon energy is by simple grating rotation. Again, due to the high power density, the gratings are manufactured from Glidcop and employ an integrally cooled structure (DiGennaro & Swain, 1990a). The size and mass of these optical elements meant that the normally used mounting schemes could not be used, and a new system of kinematically mounting the elements using a miniature version of the six-strut approach was used. In addition, a further level of complexity was necessary in order to obtain stress-free mounting, even with the need for water cooling and guard vacuum connections. A prototype of this new type of arrangement was constructed and successfully installed and tested on beamline 6 at SSRL (Heimann *et al.*, 1990). The exit slits of the monochromator move along the optical axis to allow 0.75 m of motion to track the monochromatic focal plane as a function of wavelength. The slits are again of a flexural pivot design but in this case are uncooled, and the whole assembly is mounted to the floor on Invar struts.

Following the exit slits, the beam diverges in the vertical plane, and in the horizontal plane continues to diverge from the source. The refocusing optics image the source in the horizontal direction, and the moveable exit slit in the vertical direction, to a fixed image position. The experiments on this beamline all require a small focused spot size and in some cases the focus position is the location of the object aperture of an X-ray microscope. A varying image position in this case would cause a severe loss of flux. In order to compensate for the large range of motion of the exit slit, the vertical focus mirror can

be bent into a range of radii by the application of a load from a piezo driver. The mirror is shown in Fig. 4 and is based on the design of Howells & Lunt (1993), in which the thickness of the mirror varies as the cube root of the distance from each end. This section is produced by wire electric discharge machining, and this is also used to provide flexural hinges at each end to allow rotation, and in the center to convert translation of the piezo parallel to the mirror to a perpendicular motion. The piezo can be programmed to give a radius appropriate to any particular position of the exit-slit stage. Measurements of the radius of the mirror using a long trace profiler (LTP) (Irick, 1992; Irick, McKinney, Lunt & Tackacs, 1992) showed that the residual slope errors over the range of radii needed were less than $5\ \mu\text{rad}$. Measurements of a $10\ \mu\text{m}$ exit slit give a measured image size of less than $20\ \mu\text{m}$ (FWHM) (Warwick & Shlezinger, 1994). The light diverging from the source in the horizontal direction is refocused at 14:1 demagnification by one of two glass mirrors into its appropriate end station line. The mirrors are interchanged by lateral translation and allow a time-sharing mode of operation between the two end stations. The arrangement of the beamline, showing the refocus optics in the foreground, is given in Fig. 5. The measured focus size in the horizontal direction is $45\ \mu\text{m}$ (FWHM), in agreement with predictions.

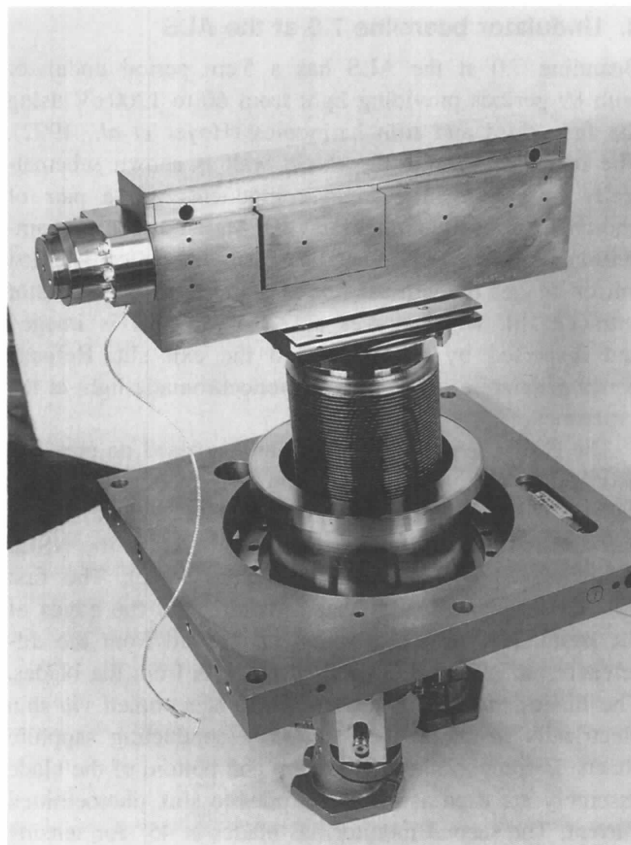


Figure 4

Piezo-driven bendable vertical refocusing mirror showing the wire electric discharge machined slots defining the cube-root relation between thickness and distance from each end.

The theoretical flux output from the beamline is shown in Fig. 6 for a resolving power of 10^4 . It can be seen that even at this very high resolving power, resolved fluxes of around 10^{13} s^{-1} are predicted for the low-energy region up to 200 eV, and over 10^{12} s^{-1} up to 800 eV. Crucial in achieving this throughput are low micro-roughness reflecting surfaces and high-diffraction-efficiency gratings. The development of these components to the point where $0.5 \mu\text{rad}$ slope errors and micro-roughnesses of less than 3 \AA have been achieved has taken several years, and these efforts are reported by McKinney *et al.* (McKinney, Irick & Lunt, 1992; McKinney, 1994).

The beamline was first commissioned with beam in March 1994. In initial measurements, the beam size on the entrance slit was measured to be less than $10 \mu\text{m}$, as expected. Also, the focused beam size at the sample was less than $50 \mu\text{m}$, and the resolving power was in agreement with theory. An example of the resolution that is routinely available is shown in Fig. 7, which shows the $1s - \pi^*$ *K*-edge region of nitrogen gas, and indicates a resolving power in excess of 8×10^3 . In addition, the beam stability using the PBPMs was shown to be better than $5 \mu\text{m}$ at the source over the course of an 8 h shift without resorting to active feedback (Warwick, 1994). Using the PBPMs and the storage-ring pick-up monitors, the effect of the integrated fields of the undulator on the position of the electron beam have been measured, and a compensation scheme using

the steering correctors in each straight now allows user operation of the undulator. Coordinated scanning of the monochromator and the undulator has also been successfully demonstrated. A full description of the beamline and performance is given by Warwick, Heimann, Mossessian, McKinney & Padmore (1994), and presentation of some of the first scientific measurements is also given by Denlinger *et al.* (1994). Because of the high quality of the beamline engineering and the optics design and fabrication, the beamline has required minimal commissioning, and within days of first having beam in the monochromator the first scientific program was underway.

5. Future possibilities

Although beamline 7.0 has performed to its original specification, there are significant opportunities for further improvement on this design. A review of all of the possibilities is beyond the scope of this paper, but the reader is directed to the reviews by Peatman & Senf (1993), by Reininger (1992), and to the proceedings of a workshop on high-performance monochromators, held at BESSY in 1991. Variable included-angle designs such as the SX700 used with a spherical focusing mirror and the focusing SGM (F-SGM) offer tremendous flexibility in comparison to the standard fixed included-angle SGM design. They also offer the potential of a significant increase in throughput if

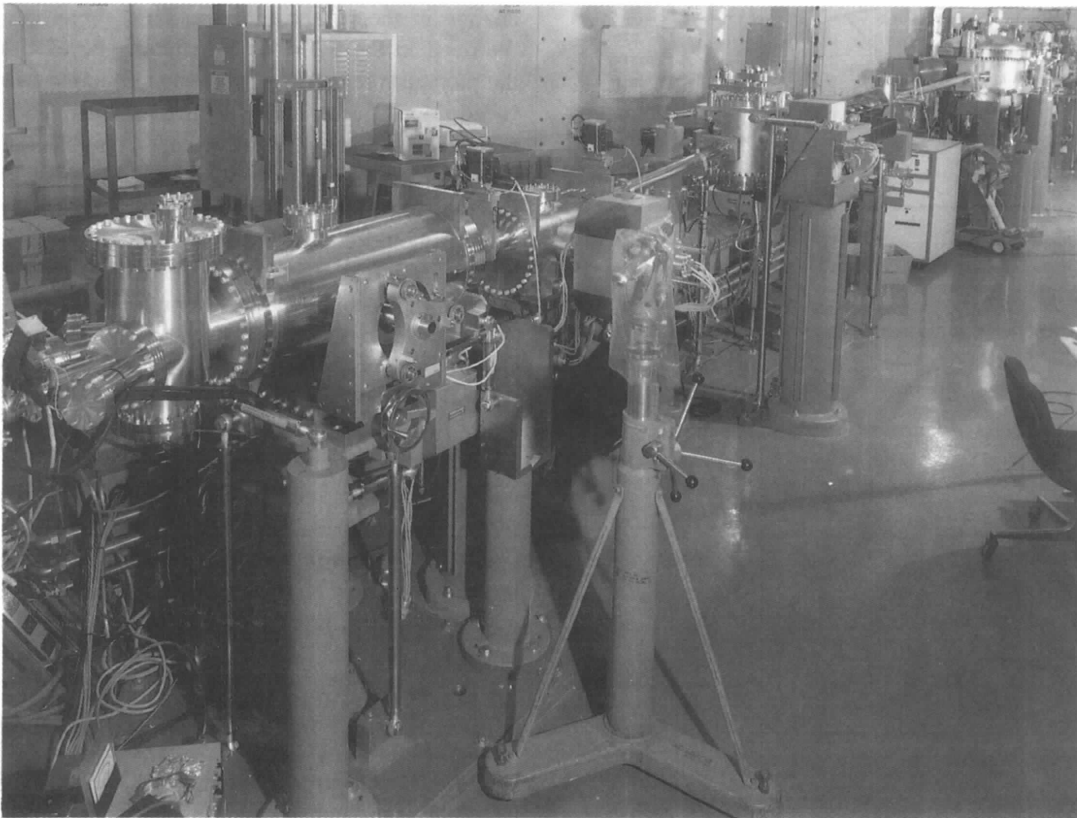


Figure 5
Beamline 7.0, showing the refocus mirror tank in the foreground and the monochromator in the background.

optimum grating parameters are chosen. One of the benefits of a source such as an ALS undulator, in which the phase space occupied by the source in the vertical direction is nearly diffraction limited throughout the soft X-ray energy range, is the opportunity to produce a very small beam size at the entrance slit of a monochromator, thus reducing the necessity of having a high line density in order to achieve a high spectral resolution. As shown by Padmore, Martynov & Hollis (1993), the use of an optimum included angle, with optimum grating groove width and depth, and an appropriate reflection coating, can give very significant increases in diffraction efficiency. In the case of the ALS, for example, the vertical beam size is less than $100\ \mu\text{m}$ FWHM, and combined with the excellent stability of the source, we therefore have the opportunity to build entrance-slitless designs offering high resolution with relatively low line densities, and hence significantly improved throughput. In order to optimize the performance over a reasonable energy range a variable angle configuration could be used, together with a lateral translation mechanism for the grating that allowed the selection of the appropriate groove depth from a laterally graded groove-depth grating (Padmore *et al.*, 1993). Other designs show promise, especially the constant-length monochromator of Ishiguro *et al.* (1989), originally used as a VUV monochromator on an undula-

tor at UVSOR, and under consideration as a soft X-ray monochromator on BESSY 2 (Peatman & Senf, 1993). This is an SGM in which a fixed-plane mirror is added after the grating so that a parallel in-out geometry can be used, and a solution of the focusing equation can be found simply by varying the image and object distance whilst keeping the sum of the image and object distance fixed. Practically, this is achieved by mounting the plane mirror-spherical grating combination on a common table that is moved between the fixed entrance and exit slits. The geometry almost satisfies the Rowland-circle condition and should be capable of very high resolution with a high dispersive aperture. A further modification of the variable angle geometry has been suggested by Li-Jun, Cocco & Jark (1994), in which a cylindrical pre-mirror is used to form a converging beam onto a plane grating. By correct choice of the pre-mirror and grating angles, the system can be in focus for fixed-slit positions, and offer excellent higher order rejection capabilities. It is interesting that this is essentially a reversed version of the monochromator of Miyake, Kato & Yamashita (1969), and that a system based on that design by Howells, Norman, Norman & West (1978) has previously been used in this mode (Padmore, 1986*a,b*). Another separate direction that is being pursued is the use of variable line space gratings (VLS) in convergent light (Hettrick & Bowyer, 1983; Hettrick & Underwood, 1986). The main merit of this type of design is that the focal plane is almost perpendicular to the principal ray and thus rotation of the grating to change wavelength causes only a negligible change in the image distance. This, therefore, overcomes the need in the SGM for translating the exit slits to track the monochromatic focal plane as a function of wavelength. In addition, higher order aberrations can be significantly reduced over extended wavelength ranges compared with fixed line density designs. The article by McKinney (1992) gives a full review of the theory of VLS gratings.

A further exciting possibility offered by the converging-light VLS design is that the exit plane is almost flat and so it offers the possibility of performing dispersed spectroscopy. A simple example would be one in which the transmission spectrum through a thin foil was to be measured as a function of time. Conventional designs rely on mechanical scanning and so are therefore slow. The thin foil could be put in the flat field plane so that there would be a correlation between position and wavelength on the foil. The variation of transmitted intensity with position and hence wavelength could be monitored with a photodiode array which could be read out at intervals to give the absorption spectrum as a function of time. Another version of this arrangement could be used with a solid sample from which the position dependence of the electron yield could be imaged with a small electrostatic lens system. The significance of the VLS arrangement is that it gives us the possibility of time-resolved high-resolution soft X-ray spectroscopy. For example, the bandpass of the U5 undulator at the carbon *K* edge of 4 eV would give us the opportunity to measure a section of the near-edge X-ray absorption region and,

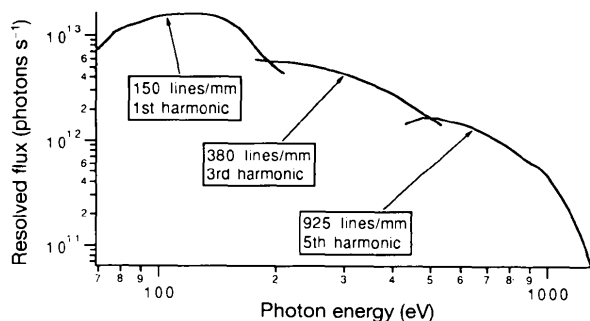


Figure 6
Computed flux at the sample for a resolving power of 10^4 .

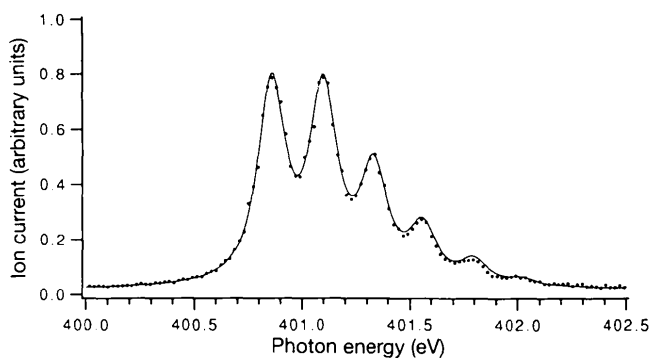


Figure 7
Nitrogen *K*-edge region for gaseous nitrogen showing the $1s-\pi^*$ resonance with vibrational fine structure. The monochromator bandpass determined from this data yield a resolving power of >8000 .

for example, could give us molecular information during surface reactions with sub-millisecond time resolution.

6. Conclusions

Beamline 7.0 currently represents the state of the art in undulator-based soft X-ray monochromators. The combination of the ultra-high brightness of the ALS undulators with a high-performance monochromator opens up completely new opportunities in soft X-ray science. The successful completion of beamline 7.0 has been the result of a combined program over the last five years in monochromator design, high-power engineering and optical fabrication, and has resulted in a system that achieved its design specification from the start of operation.

Clearly, there are opportunities for specialized designs that will offer even higher performance for particular experiments. One of these is X-ray microscopy where there is the opportunity for significant benefit from the use of low-dispersion entrance-slitless monochromator designs. Many avenues of investigation have been opened up by the advent of third-generation undulator-based sources of soft X-rays; beamline 7.0 has shown that very significant technological problems in utilizing the radiation can be overcome, ensuring a brilliant future for the new science of spectromicroscopy.

The development of beamline 7.0 at the ALS represents the work of many people over a number of years. We would like to mention here in particular Dick DiGennaro who guided the mechanical design, Tony Catalano who looked after the installation, the survey and alignment crew under Ted Lauritsen, Wayne McKinney who was responsible for the program to develop ALS water-cooled optics, Phil Heimann who jointly worked on the optical design and helped with commissioning, and Malcolm Howells who worked out the original concept for the beamline. We would also like to thank Bill Peatman and Werner Jark for many illuminating discussions on monochromator design. This work was supported by the Director, Office of Energy Research, Office of Basic Energy Sciences, Materials Sciences Division of the US Department of Energy, under Contract No. DE-AC03-76SF00098.

References

- Avery, R. T. (1984). *Nucl. Instrum. Methods*, **222**, 146–158.
- Buckley, C., Rarback, H., Alforque, R., Shu, D., Ade, H., Hellman, S., Iskander, N., Kirz, J., Lindaas, S., McNulty, I., Oversluisen, M., Tang, E., Attwood, D., DiGennaro, R., Howells, M., Jacobsen, C., Vladimirovsky, Y., Rothman, S., Kern, D. & Sayre, D. (1989). *Rev. Sci. Instrum.* **60**(7), 2444–2447.
- Chen, C. T. (1987). *Nucl. Instrum. Methods*, **A256**, 595–604.
- Chen, C. T. & Sette, F. (1989). *Rev. Sci. Instrum.* **60**, 1616–1621.
- Chen, C. T. & Sette, F. (1990). *Phys. Scr.* **T31**, 119–126.
- Denlinger, J. D., Rotenberg, E., Warwick, T., Visser, G., Nordgren, J., Guo, J.-H., Skytt, P., Kevan, S. D., McCutcheon, K. S., Shu, D., Bucher, J., Edelstein, N., Tobin, J. G. & Tonner, B. P. (1994). *Rev. Sci. Instrum.* Submitted.
- Dietrich, H. & Kunz, C. (1972). *Rev. Sci. Instrum.* **43**, 434–442.
- DiGennaro, R., Gee, B., Guigli, J., Hogrefe, H., Howells, M. & Rarback, H. (1988). *Nucl. Instrum. Methods*, **A266**, 498–506.
- DiGennaro, R. & Swain, T. (1990a). *Nucl. Instrum. Methods*, **A291**, 305–312.
- DiGennaro, R. & Swain, T. (1990b). *Nucl. Instrum. Methods*, **291**, 313–318.
- Domke, M., Mandel, T., Puschmann, A., Xue, C., Shirley, D. A., Kaindl, G., Petersen, H. & Kuske, P. (1992). *Rev. Sci. Instrum.* **63**, 80–89.
- Heimann, P. A., Senf, F., McKinney, W., Howells, M., van Zee, R. D., Medhurst, L. J., Lauritzen, T., Chin, J., Meneghetti, J., Gath, W., Hogrefe, H. & Shirley, D. A. (1990). *Phys. Scr.* **T31**, 127–130.
- Hettrick, M. C. & Bowyer, S. (1983). *Appl. Opt.* **22**, 3921–3924.
- Hettrick, M. C. & Underwood, J. (1986). *AIP Conf. Proc.* **147**, 237–245.
- Hogrefe, H., Howells, M. R. & Hoyer, E. (1986). *SPIE J.* **733**, 274–285.
- Howells, M. R. & Lunt, D. (1993). *Opt. Eng.* **32**(8), 1981–1989.
- Howells, M. R., Norman, D., Norman, G. P. & West, J. B. (1978). *J. Phys. E*, **11**, 199–202.
- Hoyer, E., Chin, J., Halbach, K., Hassenzahl, W. V., Humphries, D., Kincaid, B., Lancaster, H. & Plate, D. (1992). *Rev. Sci. Instrum.* **63**(1), 359–362.
- Irick, S. C. (1992). *Rev. Sci. Instrum.* **63**(1), 1432–1435.
- Irick, S. C., McKinney, W. R., Lunt, D. L. & Tackacs, P. Z. (1992). *Rev. Sci. Instrum.* **63**(1), 1436–1438.
- Ishiguro, E., Suzuki, M., Yamazaki, J., Nakamura, E., Sakai, K., Matsudo, O., Mizutani, N., Fukui, K. & Watanabe, M. (1989). *Rev. Sci. Instrum.* **60**, 2105–2108.
- Jark, W. (1992). *Rev. Sci. Instrum.* **63**, 1241–1246.
- Jark, W. & Melpignano, P. (1994). *Nucl. Instrum. Methods*. In the press.
- Johnson, E. & Oversluisen, T. (1989). *Rev. Sci. Instrum.* **60**, 1947–1950.
- Kaindl, G., Domke, M., Laubschat, C., Weschke, E. & Xue, C. (1992). *Rev. Sci. Instrum.* **63**(1), 1234–1240.
- Kunz, C., Haensel, R. & Sonntag, B. (1968). *J. Opt. Soc. Am.* **58**, 1415–1421.
- Larsson, C. U. S., Federman, F., Beutler, A., Rieck, A., Verbin, S. & Moeller, T. (1992). *Hasylab Annu. Rep.* pp. 100–105.
- Li-Jun, L., Cocco, D. & Jark, W. (1994). *Nucl. Instrum. Methods*. In the press.
- Lu, L.-J. & Chen, J.-Y. (1991). *Nucl. Instrum. Methods*, **A309**, 581–584.
- McKinney, W. R. (1992). *Rev. Sci. Instrum.* **63**(1), 1410–1414.
- McKinney, W. R. (1994). *Nucl. Instrum. Methods*. In the press.
- McKinney, W. R., Irick, S. C. & Lunt, D. L. J. (1992). *Nucl. Instrum. Methods*, **A319**, 179–184.
- Maezawa, H., Nakai, S., Mitani, S., Noda, H., Namioka, T. & Sasaki, T. (1986). *Nucl. Instrum. Methods*, **A246**, 310–313.
- Miyake, K. P., Kato, R. & Yamashita, H. (1969). *Sci. Light*, **18**, 39–56.
- Mortazavi, P., Woodle, M., Rarback, H., Shu, D. & Howells, M. (1986). *Nucl. Instrum. Methods*, **A246**, 389–393.
- Muramatsu, Y., Kato, H., Maezawa, H. & Harada, T. (1992). *Rev. Sci. Instrum.* **63**(1), 1305–1308.
- Muramatsu, Y. & Maezawa, H. (1989). *Rev. Sci. Instrum.* **60**(7), 2078–2080.
- Mythen, C. S., van der Laan, G. & Padmore, H. A. (1992). *Rev. Sci. Instrum.* **63**, 1313–1316.
- Namioka, T., Noda, H., Goto, K. & Katayama, T. (1983). *Nucl. Instrum. Methods*, **208**, 215–222.
- Nataletti, P., Contarini, S., Gariazzo, C., Minnaja, N., Musicanti, M., Jark, W., Kiskinova, M., Melpignano, P., Morris, D. & Rosei, R. (1992). *Surf. Interface Anal.* **18**, 655–660.
- Nyholm, R., Svensson, S., Nordgren, J. & Flodstrom, A. (1986). *Nucl. Instrum. Methods*, **A246**, 267–271.

- Padmore, H. A. (1986a). Technical Report DL/SCI/TM45E. Daresbury Laboratory, Warrington, England.
- Padmore, H. A. (1986b). *SPIE J.* **733**, 253–261.
- Padmore, H. A. (1989). *Rev. Sci. Instrum.* **60**, 1608–1615.
- Padmore, H. A. (1991). *Proceedings of the International Workshop on High Performance Monochromators and Optics for Synchrotron Radiation in the Soft X-ray Region*, BESSY, Berlin, 26–28 March 1991.
- Padmore, H. A., Martynov, V. & Hollis, K. (1993). *Nucl. Instrum. Methods*. In the press.
- Peatman, W. B., Bahrtdt, J., Eggenstein, F. & Senf, F. (1991). *BESSY Annu. Rep.* pp. 471–477.
- Peatman, W. B., Bahrtdt, J., Gaupp, A., Scafers, F. & Senf, F. (1992). *BESSY Annu. Rep.* pp. 499–505.
- Peatman, W., Carbone, C., Gudat, W., Heinen, W., Kusks, P., Pfluger, J., Schafers, F. & Schroeter, T. (1989). *Rev. Sci. Instrum.* **60**(7), 1445–1450.
- Peatman, W. B. & Senf, F. (1993). *Vacuum Ultraviolet Radiation Physics, Proceedings of the Tenth VUV Conference*, Paris, 27–31 July 1993, edited by F. J. Wuillemeir, Y. Petroff & I. Nenner. Singapore: World Scientific.
- Petersen, H. (1982). *Opt. Commun.* **40**, 402–407.
- Petersen, H. (1986). *Nucl. Instrum. Methods*, **A246**, 260–263.
- Petersen, H., Haase, J., Puschmann, A., Reimer, A. & Treichler, R. (1983). *Ann. Isr. Phys. Soc.* **6**, 57–60.
- Petersen, H., Jung, C., Hellwig, C., Peatman, W. & Gudat, W. (1992). *BESSY Annu. Rep.* pp. 494–498.
- Petersen, H., Jung, C., Hellwig, C., Peatman, W. & Gudat, W. (1994). *Rev. Sci. Instrum.* Submitted.
- Randall, K. J., Eberhardt, W., Feldhaus, J., Erlebach, W., Bradshaw, A. M., Xu, Z., Johnson, P. D. & Ma, Y. (1992). *Nucl. Instrum. Methods*, **A319**, 101–105.
- Randall, K. J., Feldhaus, J., Erlebach, W., Bradshaw, A. M., Eberhardt, W., Xu, Z., Ma, Y. & Johnson, P. D. (1992). *Rev. Sci. Instrum.* **63**(1), 1367–1370.
- Reimer, F. & Torge, R. (1983). *Nucl. Instrum. Methods*, **208**, 313–315.
- Reininger, R. (1992). *Nucl. Instrum. Methods*, **A319**, 110–115.
- Reininger, R. & Saile, V. (1990). *Nucl. Instrum. Methods*, **A288**, 343–348.
- Senf, F., Berens, K., Rautenfeldt, V., Cramm, S., Kunz, C., Lamp, J., Saile, V., Schmidt-May, J. & Voss, J. (1986). *Nucl. Instrum. Methods*, **A246**, 314–319.
- Smither, R. K., Foster, G. A., Bilderback, D. H., Bedzyk, M., Finkelstein, K., Henderson, C., White, J., Merman, L. E., Stefan, P. & Oversluizen, T. (1989). *Rev. Sci. Instrum.* **60**(7), 1486–1492.
- Warwick, T. (1994). *Rev. Sci. Instrum.* In the press.
- Warwick, T. & Heimann, P. (1992). *Nucl. Instrum. Methods*, **A319**, 77–82.
- Warwick, T., Heimann, P., Mossessian, D., McKinney, W. & Padmore, H. A. (1994). *Rev. Sci. Instrum.* In the press.
- Warwick, T. & Shlezinger, M. (1994). *Rev. Sci. Instrum.* In the press.
- Warwick, T., Shu, D., Rodricks, B. & Johnson, E. D. (1992). *Rev. Sci. Instrum.* **63**, 550–553.
- Yagashita, A., Masui, S., Toyoshima, T., Maezawa, H. & Shigemasa, E. (1992). *Rev. Sci. Instrum.* **63**(1), 1351–1354.